Journal of Organometallic Chemistry, 426 (1992) 331–342
Elsevier Sequoia S.A., Lausanne
JOM 22234

A study of polarities, polarisabilities and infrared spectra of $LM(CO)_5$ complexes (M = Cr, Mo or W; L = trimethylamine, quinuclidine, pyridine, *p*-methyl- or *p*-t-butylpyridine) and of the X-ray crystal structure of quinuclidine-$Cr(CO)_5$: evidence for π-acceptor behaviour of coordinated pyridine

M.J. Aroney, R.M. Clarkson, T.W. Hambley and R.K. Pierens

Department of Inorganic Chemistry, University of Sydney, Sydney, NSW 2006 (Australia)

(Received June 24, 1991)

Abstract

Carbonyl infrared frequencies, electric dipole moments and optical polarisability anisotropies of pyridine and of *p*-methyl and *p*-t-butyl-pyridine-$M(CO)_5$ complexes (M = Cr, Mo or W) are compared with the corresponding parameters for the analogous trimethylamine and quinuclidine-$M(CO)_5$ complexes. For the same ligand L in $LM(CO)_5$, the sequence of $\nu(CO)A_1$ is $Cr < W \leqslant Mo$. The carbonyl bands are only slightly affected by variation in L or M in the complexes studied. Trends in the molecular dipole moments of the $LM(CO)_5$ complexes suggest a degree of π-acceptor capability for the bonded pyridine system but the evidence is not conclusive. Anisotropic molecular polarisabilities derived from experiment for the pyridine and *p*-substituted pyridine-$M(CO)_5$ complexes, when compared with parameters calculated for a purely σ-bonded N–M model for such systems, show a strong enhancement of polarisability specifically along the pyridine–M-*trans*(CO) axis. This is related to conjugative electron delocalisation between the pyridine and $M(CO)_5$ moieties and indicates a degree of π-bond character in the connecting N–M bond. The crystal structure of quinuclidine-$Cr(CO)_5$ is reported. Comparison of bond dimensions of this complex with those of pyridine-$Cr(CO)_5$ yields positive though qualified support for a π-component in the N–Cr bond of pyridine-$Cr(CO)_5$.

Introduction

In contrast to aliphatic amines, pyridine has the potential to act as a π-acid through its π^*-antibonding orbitals. It has been suggested, however, that if pyridine is to π-bond at all, it will do so to a limited extent [1]. Many techniques have been applied to probing the nature of the metal–pyridine interaction [2–16] but the importance of π-bonding remains a contentious issue. A new approach is now applied in which molecular polarisability anisotropies are determined for

---

Correspondence to: M.J. Aroney, Department of Inorganic Chemistry, University of Sydney, Sydney, NSW 2006, Australia.

pyridine-M(CO)$_5$ complexes and compared with the analogous parameters found for trimethylamine and quinuclidine-M(CO)$_5$ complexes (M = Cr, Mo or W). Comparative studies of the electric dipole moments, infrared active carbonyl vibrational modes and bond dimensions are also presented.

Experimental

The complexes were synthesised by published methods [7,17–19] and were purified to recognised criteria of purity (m.p., IR, ^{1}H NMR, mass spectra and C,H,N analysis in the case of the quinuclidine complexes); melting points of 116–117, 121–122 and 133–134 °C were found for quinuclidine-M(CO)$_5$ in which M is Cr, Mo and W, respectively.

Electric dipole moments μ and molar Kerr constants $_{\mathrm{m}}K$ were determined in cyclohexane solution at 298 K; the experimental procedures and treatment of the measured data are given in refs. 20–22. The preparation and handling of solutions were carried out in an atmosphere of dry nitrogen. Reliable measurements could not be obtained for Me$_3$NMo(CO)$_5$ because of instability of its solution in the dielectric cell. Infrared spectra were recorded on a Digilab FTS 80/20 Fourier transform infrared spectrometer.

The crystal structure of quinuclidine-Cr(CO)$_5$ was determined. For the diffractometry, the crystal was mounted on a glass fibre with cyanoacrylate resin. Lattice parameters at 21 °C were determined by a least-squares fit to the setting parameters of 25 independent reflections, measured and refined on an Enraf–Nonius CAD4F four-circle diffractometer employing graphite monochromated Mo-K_α radiation.

Crystal data. Formula C$_{12}$H$_{13}$CrNO$_5$; M 303.24, tetragonal, space group $I\bar{4}2d$, a 13.645(1), c 14.866(2) Å, $Z = 8$, V 2767.8 Å^3, D_c 1.455 g cm^{-3}, μ(Mo-K_α) 7.90 cm^{-1}, λ (Mo-K_α) 0.7107 Å, $F(000)$ 1248 electrons.

Structure determination

Intensity data were collected in the range $1.0 < \theta < 25.0°$ using an ω–1.33θ scan. The scan widths and horizontal counter apertures employed were $(1.00 + 0.34 \tan \theta)°$ and $(2.70 + 1.05 \tan \theta)$ mm. Data reduction and application of Lorentz, polarisation and absorption corrections were carried out using the Enraf–Nonius Structure Determination Package [23]. Of the 1028 independent non-zero reflections collected, 884 with $I > 2.5\sigma(I)$ were considered observed and used in the calculations.

The structure was solved by Patterson methods using SHELX-76 [24] which enabled the location of the Cr atom and the solution was extended by difference Fourier methods. The location of the quinuclidine ligand on the two-fold axis means it is disordered. An additional level of disorder was also found; two sites for each of the bridging C atoms with occupancies 0.54 : 0.46 successfully modelled the observed electron density. Hydrogen atoms were included at sites calculated assuming tetrahedral geometries and C–H bond lengths of 0.97 Å with isotropic thermal parameters. The contributors to the disordered ligand atoms were refined isotropically and all other atoms were refined anisotropically.

Full-matrix least-squares refinement of an overall scale factor, positional and thermal parameters converged (all shifts $< 0.08\sigma$) with R * = 0.036, $R_w = 0.040$

Table 1

Infrared carbonyl stretching frequencies (cm^{-1}) for (amine)$M(CO)_5$ complexes in n-hexane [a]

Complex	A_{1eq}	A_{1ax}	B_1	E
trimethylamine-$Cr(CO)_5$ [b]	2065	1917		1944
trimethylamine-$Mo(CO)_5$ [b]	2072	1921		1941
trimethylamine-$W(CO)_5$	2072	1919	1984	1930
quinuclidine-$Cr(CO)_5$	2066	1915	1987	1933
quinuclidine-$Mo(CO)_5$	2073	1918	1990	1937
quinuclidine-$W(CO)_5$	2071	1916		1928
pyridine-$Cr(CO)_5$	2069	1921	1988	1940
p-methylpyridine-$Cr(CO)_5$	2069	1919		1939
p-t-butylpyridine-$Cr(CO)_5$	2068	1918		1939
pyridine-$Mo(CO)_5$	2074	1923	1990	1944
pyridine-$W(CO)_5$	2073	1921		1934

[a] Uncertainty in the present measurements of ν is ± 0.5 cm^{-1}. [b] Infrared spectrum not determined; the data are quoted from ref. 19.

and $w = 1.27/(\sigma^2(F_o) + 0.000732F_o^2)$. Maximum excursions in a final difference map were +0.24 and −0.32 e $Å^{-3}$. Scattering factors and anomalous dispersion terms used for Cr were taken from the International Tables [25] and for all other atoms the values supplied in SHELX-76 were used [24]. All calculations were carried out using SHELX-76 [24] and plots were drawn using ORTEP [26].

The atom-numbering scheme is given in Fig. 1. Final atomic coordinates, bond lengths and bond angles are listed in Tables 6–8. Listings of observed and calculated structure factors, hydrogen atom coordinates and thermal parameters (Tables S1–S3) are available from the authors.

Results and discussion

Infrared spectra

The amine-$M(CO)_5$ complexes have local C_{4v} symmetry with respect to the $M(CO)_5$ moiety. Three infrared active vibrational modes are allowed [27], two A_1 and an E. For some of the complexes the activation of the infrared forbidden B_1 mode is apparent. This can be rationalised in terms of the bending of the equatorial carbonyl ligands slightly out of the plane causing a transverse dipole moment to be activated [28], and of asymmetry of the amine ligand [2].

It has been suggested that the A_1 band is more sensitive to L–M π-bonding variations than the E or A_2 bands [29]. Comparison of the $\nu(CO)A_1$ bands in Table 1 shows that they are not much affected by variation of the ligand L; the $\nu(CO)A_1$ values for the pyridine complexes are marginally greater than those of the trimethylamine and quinuclidine complexes. For the same ligand L in $LM(CO)_5$, the trend observed in $\nu(CO)A_1$ is $Cr < W \leqslant Mo$. A similar order has been reported for (η^6-arene)$M(CO)_3$ complexes [30]. Changes of L or M in $LM(CO)_5$ could affect σ-polarisation of the $M \leftarrow CO$ bond, π-back bonding (electron drift from M to CO) and π-forward bonding (electron drift from CO to M); these factors are discussed in refs. 31 and 32. It appears from the small differences

---

* $R = \Sigma(||F_o| - |F_c||)/\Sigma|F_o|$, $R_w = (\Sigma w(|F_o| - |F_c|)^2/\Sigma wF_o^2)^{1/2}$.

Table 2

Electric dipole moments, molar Kerr constants and molecular polarisability anisotropies of solutes at infinite dilution in cyclohexane at $T = 298$ K and $\lambda = 589$ nm [a]

Solute	$10^{30}\mu$ (Cm)	$10^{27}\,{}_{\infty}({}_{m}K)$ (m^5 V^{-2} mol^{-1})	$10^{40}\Gamma$ [b] (Cm^2 V^{-1})
trimethylamine	2.46 ± 0.10 [c]	-1.9 ± 0.2 [c]	-0.64 ± 0.05
quinuclidine	3.80 ± 0.20	2.6 ± 0.2	0.36 ± 0.10
pyridine	7.10 ± 0.05	150 ± 5	5.62 ± 0.05
p-methylpyridine	8.20 ± 0.05	279 ± 9	8.0 ± 0.1
p-t-butylpyridine	8.50 ± 0.05	423 ± 7	11.3 ± 0.1
trimethylamine-$Cr(CO)_5$	16.9 ± 0.1 [d]	-1505 ± 15 [d]	-10.7 ± 0.1
trimethylamine-$W(CO)_5$	19.5 ± 0.1	-2410 ± 35	-12.8 ± 0.1
quinuclidine-$Cr(CO)_5$	19.8 ± 0.1	-1800 ± 30	-9.4 ± 0.1
quinuclidine-$Mo(CO)_5$	21.0 ± 0.1	-2165 ± 32	-9.8 ± 0.1
quinuclidine-$W(CO)_5$	21.5 ± 0.1	-2291 ± 23	-10.0 ± 0.1
pyridine-$Cr(CO)_5$	20.5 ± 0.1	580 ± 25	2.8 ± 0.1
p-methylpyridine-$Cr(CO)_5$	22.6 ± 0.1	1474 ± 16	5.8 ± 0.1
p-t-butylpyridine-$Cr(CO)_5$	22.9 ± 0.1	2136 ± 22	8.3 ± 0.1
pyridine-$Mo(CO)_5$	21.3 ± 0.1	417 ± 14	1.8 ± 0.1
pyridine-$W(CO)_5$	22.8 ± 0.2	698 ± 31	2.7 ± 0.1

[a] Dipole moments, molar Kerr constants and polarisabilities are expressed in SI units. The conversion factors from the electrostatic (c.g.s., e.s.u.) system are, respectively: 1 Cm = 0.2998×10^{30} D, 1 m^5 V^{-2} $mol^{-1} = 0.8988 \times 10^{15}$ e.s.u. mol^{-1}, 1 Cm^2 $V^{-1} = 0.8988 \times 10^{16}$ cm^3. [b] The molecular polarisability anisotropy Γ is defined as $(2b_1 - b_2 - b_3)$ throughout. [c] Experimental data from ref. 33. [d] Experimental data from ref. 34.

observed in the carbonyl stretches that the balance between such factors and, for that matter, the electron distribution associated with the bonded carbonyl groups, are little affected by variation in L or M. The infrared band positions do not provide a sensitive probe of electronic effects in the $LM(CO)_5$ complexes of this study.

Electric dipole moments

Another approach to studying electron distributions in $LM(CO)_5$ systems is by the measurement of electric dipole moments. Determinations made in the non-interacting solvent cyclohexane are listed in Table 2 which includes also measured dipole moments of the free ligands pyridine, *p*-methylpyridine, *p*-t-butylpyridine and quinuclidine. Earlier work [34] has established that for $LM(CO)_5$ complexes of this type, the dipole moment vector is directed along the N–M–CO(*trans*) axis with the *trans*-carbonyl electrically negative relative to ligand L (from aromatic solvent induced NMR shifts).

It is found that for similar M, the molecular dipole moments of the complexes decrease in the order: pyridine-$M(CO)_5$ > quinuclidine-$M(CO)_5$ > trimethylamine-$M(CO)_5$ which parallels the order for those of the free ligands: pyridine > quinuclidine > trimethylamine. The quinuclidine complexes would be expected to have somewhat larger moments relative to the analogous trimethylamine complexes because of the higher polarity of quinuclidine and the greater potential for inductive withdrawal of electrons from the bonded quinuclidine ligand. For both sets of amine-$M(CO)_5$ complexes (with quinuclidine or trimethylamine ligands) it is generally accepted that the metal–nitrogen bond is σ and does not have a significant π-component. With pyridine, however, the potential exists for π-acceptor properties in addition to σ donation from N to M. The inductive withdrawal of electrons from pyridine in the pyridine-$M(CO)_5$ complexes would tend to enhance the dipole moment, but π-back bonding from the $M(CO)_5$ group into the π^*-orbitals of pyridine would lead to a diminution. The dipole moment of pyridine is appreciably greater than that of quinuclidine. However, this difference is not reflected in the moments of the complexes with $M(CO)_5$. This may indicate that π-back bonding in the pyridine complexes is important.

The results are merely suggestive and by no means conclusive. Insertion of *p*-methyl or *p*-t-butyl substituents in pyridine-$Cr(CO)_5$ results in an augmentation of 2.1 and 2.4 ($\times 10^{-30}$ C m), respectively, which correlates with the electron-donor properties of these substituents. Descending the group (Cr to W), increases in μ are indicated but they are small. This is true for the complexes with the pure σ-donor ligands Me_3N and quinuclidine as well as for the pyridine complexes. Overall, it is seen that the molecular moments of the $LM(CO)_5$ complexes of this study are not greatly affected by variations in the nature of the L–M interaction.

Molecular anisotropic polarisabilities

The molar Kerr constants of the Me_3N and quinuclidine complexes are approximately similar but differ greatly from those of the pyridine complexes. The experimental ${}_{\mathrm{m}}K$ values are given in column 3 of Table 2. The polarisability ellipsoid associated with each of the $Me_3NM(CO)_5$ and quinuclidine-$M(CO)_5$ complexes is one of revolution with principal polarisabilities designated by $b_1 \neq b_2 = b_3$. Because of the lower symmetry of the bound pyridine ligands, the pyridine-$M(CO)_5$ complexes have $b_1 \neq b_2 \neq b_3$. In all cases, b_1 is the optical polarisability along the molecular symmetry axis which is also the direction of the molecular dipole moment vector; b_2 and b_3 are the polarisabilities in a plane perpendicular to that axis. It follows that $\mu_1 = \mu(\text{exp.})$ and $\mu_2 = \mu_3 = 0$. The molar Kerr constant for each of the molecules of Table 2 is related to the anisotropic polarisabilities by the Langevin–Born equation as modified by Le Fèvre [35]:

$$
{}_{\mathrm{m}}K = (N/810kT\epsilon_0)\Big\{({}_{\mathrm{D}}P/{}_{\mathrm{E}}P)\big[(b_1-b_2)^2+(b_2-b_3)^2+(b_3-b_1)^2\big] + (kT)^{-1}\mu^2(2b_1-b_2-b_3)\Big\} \qquad (1)
$$

where ${}_{\mathrm{D}}P$, ${}_{\mathrm{E}}P$, N, k, T and ϵ_0 refer in turn to the molar distortion polarisation, the molar electron polarisation, Avogadro's number, the Boltzmann constant, the absolute temperature and the permittivity of a vacuum. The ratios ${}_{\mathrm{D}}P/{}_{\mathrm{E}}P$ are 1.1 and 1.14 for Me_3N [33] and pyridine [36], respectively; they were taken as 1.1 for the other compounds which is a sufficiently good approximation in this work [37]. For Me_3N, quinuclidine and each of their $M(CO)_5$ complexes, an exact solution of eq. 1 can be obtained to yield $(b_1 - b_2)$. The principal polarisabilities of pyridine can be determined since two other relations in b_i, independent of eq. 1, are available from the molar electron polarisation and the depolarised Rayleigh scattering; the appropriate data and the method of calculation are detailed in ref. 36. For *p*-methyl- and *p*-t-butylpyridine, b_i and thence $\Sigma(b_i - b_j)^2$ can be closely assessed by adjusting the experimental b_i values of pyridine to take account of the directional polarisability increments resulting from methyl or t-butyl substitution as in ref. 38. This allows the molecular anisotropy Γ, defined in this work as $(2b_1 - b_2 - b_3)$, to be evaluated from the measured molar Kerr constant of each compound. A similar procedure is used to allow for the $\Sigma(b_i - b_j)^2$ term of eq. 1 for the pyridine or *p*-substituted pyridine-M(CO)$_5$ compounds using b_i data from the appropriate Me$_3$NM(CO)$_5$ complex and the pyridine ligand. Uncertainties in the estimation of $\Sigma(b_i - b_j)^2$ by such methods are of virtually no consequence since for these highly dipolar substances, the first term of eq. 1 is very small relative to the second term (e.g. ca. 1.5% in the case of $C_5H_5NCr(CO)_5$).

The small Γ values for Me$_3$N and quinuclidine show that each of these molecules is near isotropically polarisable. On complexation with the metal pentacarbonyl moiety, the Γ values become large and negative indicating that in the Me$_3$N and quinuclidine-M(CO)$_5$ complexes, the metal–nitrogen bond axis corresponds to the direction of minimum molecular polarisability. Small increases in $|\Gamma|$ are observed going down the group from Cr to W. Positive values of Γ for the pyridine-M(CO)$_5$ complexes indicate that in each case the metal–nitrogen bond axis is coincident with the direction of maximum polarisability; this is not unexpected since the highly polarisable b_1 axis of the bound pyridine ligand is collinear with the N–M bond. Increases in Γ following *p*-methyl or *p*-t-butyl substitution in pyridine-Cr(CO)$_5$ parallel closely the corresponding changes in the unbound ligands. Change of M in pyridine-M(CO)$_5$ results in minor variations in Γ with an apparent irregularity for the Mo complex.

More meaningful analysis is afforded by comparison of the experimental anisotropies of pyridine-M(CO)$_5$ complexes with Γ(calc.) values predicted for a σ-bonded metal–nitrogen model. For example, Γ(calc.) for pyridine-Cr(CO)$_5$ can be estimated to a reasonable approximation as Γ(exp.)quinuclidine-Cr(CO)$_5$ − Γ(exp.)quinuclidine + Γ(exp.)pyridine. Comparisons of Γ(calc.) values so derived with molecular anisotropies from experiment are given in Table 3.

The differences $\Delta\Gamma$ between the observed and calculated molecular anisotropies are large, being of the order of ca. 6–9($\times 10^{-40}$ C m^2 V^{-1}) and far in excess of the estimated uncertainty in $\Delta\Gamma$($\pm 1 \times 10^{-40}$ C m^2 V^{-1}). The results show that for all of the pyridine complexes examined, bonding between the pyridine system and the M(CO)$_5$ moiety leads to a strong enhancement of polarisability along the pyridine–M-*trans*(CO) axis above that predicted for a model in which the two "isolated" groupings are connected by a purely σ metal–nitrogen bond. It is known that for

Table 3

Comparison of molecular polarisability anisotropies from experiment Γ(exp.) with values Γ(calc.) derived on the basis of a σ-bonded metal–nitrogen model

Complex	$10^{40}\Gamma$(exp.) (C m^2 V^{-1})	$10^{40}\Gamma$(calc.) [a] (C m^2 V^{-1})	$10^{40}\Delta\Gamma$ = $10^{40}[\Gamma$(exp.) − Γ(calc.)] (C m^2 V^{-1})
pyridine-Cr(CO)$_5$	2.8	−4.2(−4.4)	7.0(7.2)
p-methylpyridine-Cr(CO)$_5$	5.8	−1.8(−2.1)	7.6(7.9)
p-t-butylpyridine-Cr(CO)$_5$	8.3	+1.5(+1.2)	6.8(7.1)
pyridine-Mo(CO)$_5$	1.8	−4.5	6.3
pyridine-W(CO)$_5$	2.7	−4.7(−6.6)	7.4(9.3)

[a] The Γ(calc.) values listed in column 3 were derived from Γ(exp.) of quinuclidine-M(CO)$_5$ complexes; those derived from Γ(exp.) of Me$_3$NM(CO)$_5$ complexes are given in parentheses.

Table 4

Principal polarisabilities b_i of trimethylamine and quinuclidine-M(CO)$_5$ complexes from experiment [a,b]

Complex	$10^{40}b_1$(exp.) ($\mathrm{C\,m^2\,V^{-1}}$)	$10^{40}b_2$(exp.) = $10^{40}b_3$(exp.) ($\mathrm{C\,m^2\,V^{-1}}$)
trimethylamine-Cr(CO)$_5$	24.1	29.5
trimethylamine-W(CO)$_5$	26.4	32.8
quinuclidine-Cr(CO)$_5$	30.3	35.1
quinuclidine-Mo(CO)$_5$	32.8	37.8
quinuclidine-W(CO)$_5$	33.1	38.1

[a] Uncertainty in the b_i values is $\pm 0.1\times 10^{-40}$ C m^2 V^{-1}. [b] The sum (b_1+2b_2) was determined from eq. 2 using $_{\mathrm{E}}P$ values of 62.8 and 69.5 cm^3 for M = Cr and W in Me$_3$NM(CO)$_5$, and 75.9, 81.9 and 82.7 cm^3 for M = Cr, Mo and W in quinuclidine-M(CO)$_5$.

delocalised electron systems, augmentations of polarisability in excess of values predicted from component segment additivity, occur along the delocalisation pathway [34,35]. The present results indicate the potential for extended delocalisation along the pyridine–M-*trans*(CO) axis and provide evidence for π-bond character in the metal–nitrogen bond. No significant trend in $\Delta\Gamma$ is apparent with *para*-substitution of methyl or t-butyl groups in the bonded pyridine ligand or with change of metal M.

To explore this further, the anisotropic molecular polarisabilities b_i were determined from the experimental Kerr constants and molar electron polarisations. The latter were derived from molecular refractivity data [39,40] on the basis that $_{\mathrm{E}}P = 0.95R_{\mathrm{D}}$. The sum Σb_i from eq. 2 was used together with Γ of Table 1 to yield b_1 and (b_2+b_3). The directional polarisabilities of the trimethylamine and quinuclidine-M(CO)$_5$ complexes (for which $b_2 = b_3$) are listed in Table 4.

$$_{\mathrm{E}}P = N(b_1+b_2+b_3)/9\epsilon_0 \qquad (2)$$

For the pyridine-M(CO)$_5$ complexes, a third relation in b_i is needed since $b_2 \neq b_3$. A procedure, sufficiently accurate for this work, involves taking b_2(complex) − b_3(complex) as equal to b_2(pyridine) − b_3(pyridine) since the bonded pyridine is primarily responsible for the difference between b_2 and b_3 of the pyridine-M(CO)$_5$ complex. The experimental b_i values are given in column 2 of Table 5. The b_i(calc.) values of column 3 are the principal polarisabilities predicted for a σ-bonded N–M model for pyridine-M(CO)$_5$, calculated as b_i(quinuclidine-M(CO)$_5$) − b_i(quinuclidine) + b_i(pyridine). The values in parentheses were independently obtained from b_i(trimethylamine-M(CO)$_5$) − b_i(trimethylamine) + b_i(pyridine). A similar procedure was used for the *p*-substituted pyridine complexes.

Comparison of the experimental and calculated b_i values in Table 5 shows that the molecular transverse polarisabilities b_2 and b_3 from experiment are close to or slightly less than the corresponding calculated values. By contrast, b_1(exp.) is in each case significantly greater than that predicted for the σ-bonded metal–nitrogen model. The results reinforce the conclusions earlier found from consideration of $\Delta\Gamma$, that the polarisability along the pyridine–M-*trans*(CO) axis is enhanced through bonding between the pyridine ligand and M beyond that expected for pure σ-bonding. The case for a significant π-bonding component in N–M is thus strengthened.

Table 5

Principal polarisabilities b_i of pyridine and *p*-substituted pyridine-M(CO)$_5$ complexes [a-d]

Complex	$10^{40}b_i$(exp.) ($C\ m^2\ V^{-1}$)	$10^{40}b_i$(calc.) ($C\ m^2\ V^{-1}$)
pyridine-Cr(CO)$_5$	$b_1 = 31.3$	28.0(27.9)
	$b_2 = 31.9$	32.2(32.2)
	$b_3 = 27.8$	28.1(28.1)
p-methylpyridine-Cr(CO)$_5$	$b_1 = 34.2$	30.8(30.7)
	$b_2 = 33.4$	34.0(34.0)
	$b_3 = 29.3$	29.7(29.7)
p-t-butylpyridine-Cr(CO)$_5$	$b_1 = 41.1$	37.6(37.5)
	$b_2 = 39.0$	38.8(38.8)
	$b_3 = 34.9$	35.1(35.1)
pyridine-Mo(CO)$_5$	$b_1 = 32.6$	30.5
	$b_2 = 33.7$	34.9
	$b_3 = 29.6$	30.8
pyridine-W(CO)$_5$	$b_1 = 32.6$	30.8(30.2)
	$b_2 = 33.3$	35.2(35.5)
	$b_3 = 29.2$	31.1(31.4)

[a] For the pyridine ligands and for the complexes, b_1 is along the molecular dipole axis; b_2 and b_3 are in the pyridine ring plane with b_3 perpendicular to that plane. [b] Molar electron polarisations were taken as 68.8, 73.2 and 86.8 cm^3 in turn for X = H, Me and t-butyl in *p*-$XC_5H_4NCr(CO)_5$ and as 72.4 and 71.9 cm^3 for Mo and W in pyridine-M(CO)$_5$. [c] Uncertainty in the b_i(exp.) values is $\pm 0.1 \times 10^{-40}$ C m^2 V^{-1}. [d] Polarisabilities $10^{40}b_i$ (C m^2 V^{-1}) for the free ligands are: $b_1 = 12.1$, $b_2 = 11.3$, $b_3 = 7.2$ (pyridine); $b_1 = 14.9$, $b_2 = 13.1$, $b_3 = 8.8$ (*p*-methylpyridine); $b_1 = 21.7$, $b_2 = 17.9$, $b_3 = 14.2$ (*p*-t-butylpyridine); $b_1 = 8.31$, $b_2 = b_3 = 8.63$ (trimethylamine); $b_1 = 14.4$, $b_2 = b_3 = 14.2$ (quinuclidine).

Table 6

Positional parameters ($\times 10^4$) for quinuclidine-Cr(CO)$_5$

Atom	*x*	*y*	*z*
Cr(1)	3729(1)	2500	1250
C(1)	5065(6)	2500	1250
O(1)	5912(4)	2500	1250
C(2)	3807(4)	2176(3)	18(3)
O(2)	3940(3)	1964(3)	−714(2)
C(3)	3785(4)	1148(4)	1544(3)
O(3)	3894(3)	334(3)	1694(3)
N(1)	2080(3)	2500	1250
C(4)	1724(16)	1921(33)	457(26)
C(5)	1679(18)	2123(44)	2110(24)
C(6)	1689(17)	3553(18)	1168(41)
C(7)	543(19)	2066(38)	367(18)
C(8)	566(15)	1891(32)	2049(19)
C(9)	534(15)	3536(16)	1345(36)
C(4′) [a]	1655(13)	2319(35)	353(12)
C(5′)	1675(14)	3402(20)	1611(28)
C(6′)	1687(14)	1639(23)	1821(24)
C(7′)	556(14)	2520(43)	367(13)
C(8′)	579(19)	3389(27)	1801(34)
C(9′)	574(16)	1535(21)	1743(30)
C(10)	167(5)	2500	1250

[a] Primes indicate disordered atoms, occ. 0.54(2).

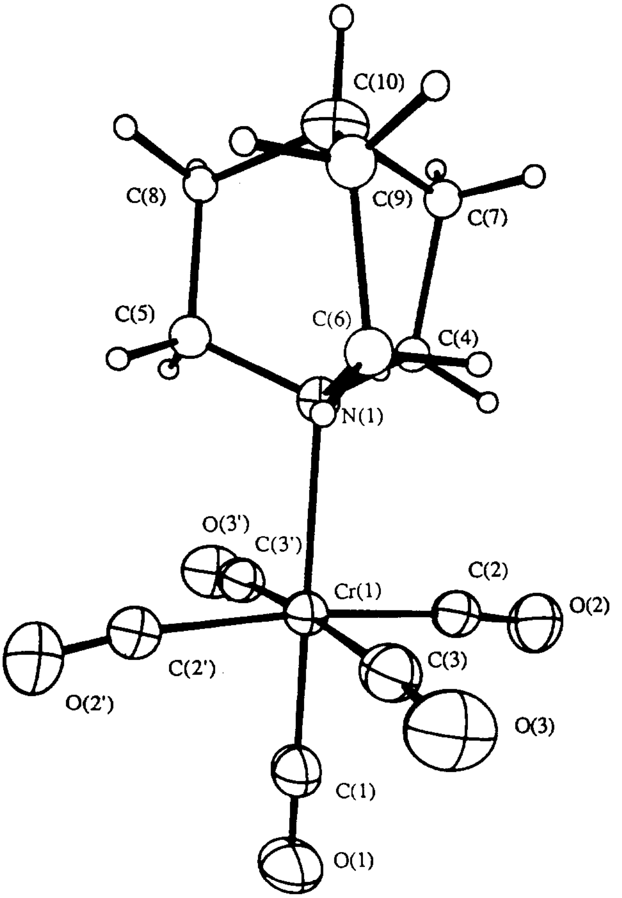

Fig. 1. An ORTEP plot of quinuclidine-Cr(CO)$_5$ showing the atom numbering scheme. Hydrogen atoms have been given arbitrary sizes, and for all other atoms 30% thermal ellipsoids are shown.

X-ray crystal structure of quinuclidine-Cr(CO)$_5$

In 1981 Cotton et al. [14] reported the coexistence of piperidine-Cr(CO)$_5$ and pyridine-Cr(CO)$_5$ in a single crystal and they stated from X-ray crystal structure studies that "the Cr(CO)$_5$N portions of the two molecular structures are extremely similar". They went on to conclude that piperidine and pyridine bind to Cr(CO)$_5$ as good σ-donors with virtually no π-acceptor interaction in either case. This was subsequently refuted by Ries et al. [15] who suggested that the crystal was in fact piperidine-Cr(CO)$_5$ occurring in disordered arrangement. Their structural studies indicated that the pyridine ligand is a weaker σ-donor and a stronger π-acceptor than the saturated piperidine analogue.

In the present work it was considered that the possibility of π-acid behaviour by pyridine in pyridine-M(CO)$_5$ could be probed by comparison of the structural parameters of this complex with those of quinuclidine-Cr(CO)$_5$. The quinuclidine ligand is less flexible than piperidine which can adopt chair or boat conformational forms.

The quinuclidine-Cr(CO)$_5$ complex is found to be an almost ideal octahedron with the largest deviation of the angles C(1)–Cr(1)–C(2) being 3.2°. The four

Table 7

Bond lengths (Å) for quinuclidine-$Cr(CO)_5$

C(1)–Cr(1)	1.824(9)	C(2)–Cr(1)	1.887(5)
C(3)–Cr(1)	1.898(6)	N(1)–Cr(1)	2.249(5)
O(1)–C(1)	1.115(11)	O(2)–C(2)	1.143(6)
O(3)–C(3)	1.142(7)	C(4)–N(1)	1.50(3)
C(5)–N(1)	1.48(3)	C(6)–N(1)	1.54(3)
C(4′)–N(1)	1.47(2)	C(5′)–N(1)	1.45(2)
C(6′)–N(1)	1.54(2)	C(7)–C(4)	1.63(4)
C(8)–C(5)	1.55(5)	C(9)–C(6)	1.50(4)
C(10)–C(7)	1.53(3)	C(10)–C(8)	1.55(3)
C(10)–C(9)	1.51(3)	C(7′)–C(4′)	1.52(4)
C(8′)–C(5′)	1.52(4)	C(9′)–C(6′)	1.53(3)
C(10)–C(7′)	1.42(2)	C(10)–C(8′)	1.57(3)
C(10)–C(9′)	1.61(3)		

equatorial CO groups have small deviations of angles such as N(1)–Cr(1)–C(2) (a result of slight steric repulsion due to the close proximity (2.39 Å) of the C(2)–O(2) carbonyl ligand to the C(4) carbon of the quinuclidine).

Some of the bond lengths for the pyridine and quinuclidine-$Cr(CO)_5$ complexes are listed in Table 9. If pyridine has appreciable π-acceptor character, a shortening of the Cr–N bond in pyridine-$Cr(CO)_5$ would be expected relative to that in quinuclidine-$Cr(CO)_5$. As well, Cr–C(*trans* to N) should be longer for the pyridine complex. The observed bond lengths bear out each of these predictions. Comparisons of CO bond distances within each complex and between the complexes are not meaningful in view of the large standard deviations. Overall, the evidence is suggestive of some π-bonding for pyridine-$Cr(CO)_5$ but it is not definitive in view of an indeterminate contribution from steric factors.

Table 8

Bond angles (°) for quinuclidine-$Cr(CO)_5$

C(2)–Cr(1)–C(1)	86.8(2)	C(3)–Cr(1)–C(1)	87.7(2)
C(3)–Cr(1)–C(2)	89.6(2)	N(1)–Cr(1)–C(1)	180.0
N(1)–Cr(1)–C(2)	93.2(2)	N(1)–Cr(1)–C(3)	92.3(2)
O(1)–C(1)–Cr(1)	180.0	O(2)–C(2)–Cr(1)	174.0(5)
O(3)–C(3)–Cr(1)	174.5(6)	C(4)–N(1)–Cr(1)	109(1)
C(5)–N(1)–Cr(1)	112(1)	C(5)–N(1)–C(4)	112(2)
C(6)–N(1)–Cr(1)	110(2)	C(6)–N(1)–C(4)	108(2)
C(6)–N(1)–C(5)	105(2)	C(4′)–N(1)–Cr(1)	113(1)
C(5′)–N(1)–Cr(1)	112(1)	C(5′)–N(1)–C(4′)	109(2)
C(6′)–N(1)–Cr(1)	110(1)	C(6′)–N(1)–C(4′)	103(2)
C(6′)–N(1)–C(5′)	108(2)	C(7)–C(4)–N(1)	108(2)
C(8)–C(5)–N(1)	112(3)	C(9)–C(6)–N(1)	109(2)
C(10)–C(7)–C(4)	108(2)	C(10)–C(8)–C(5)	106(2)
C(10)–C(9)–C(6)	109(2)	C(7′)–C(4′)–N(1)	110(2)
C(8′)–C(5′)–N(1)	116(2)	C(10)–C(7′)–C(4′)	112(2)
C(10)–C(8′)–C(5′)	105(2)	C(10)–C(9′)–C(6′)	107(2)
C(8)–C(10)–C(7)	109(2)	C(9)–C(10)–C(7)	109(2)
C(9)–C(10)–C(8)	108(2)	C(8′)–C(10)–C(7′)	110(2)
C(9′)–C(10)–C(7′)	108(2)	C(9′)–C(10)–C(8′)	106(2)

Table 9

Comparison of selected bond lengths for quinuclidine and pyridine-$Cr(CO)_5$ complexes

Bond	pyridine-$Cr(CO)_5$ [a]	quinuclidine-$Cr(CO)_5$
Cr–N	2.165(4), 2.148(4)	2.249(5)
Cr–C(*trans* to N)	1.846(6), 1.856(6)	1.824(9)
Cr–C(*trans* to CO)	1.890(4), 1.918(4), 1.893(4), 1.901(4)	1.887(5), 1.898(6)
C–O(*trans* to N)	1.152(6), 1.143(6)	1.115(11)
C–O(*trans* to CO)	1.145(4), 1.138(4), 1.132(4), 1.145(4)	1.143(6), 1.142(7)

[a] Quoted from ref. 15; the two sets of parameters for pyridine-$Cr(CO)_5$ arise from two molecules in an asymmetric unit.

Conclusions

A comparative study is presented of the infrared carbonyl vibration frequencies, electric dipole moments and optical polarisability anisotropies of pyridine and *p*-substituted pyridine-$M(CO)_5$ complexes ($M = Cr$, Mo or W) relative to the corresponding physical parameters of the analogous trimethylamine and quinuclidine-$M(CO)_5$ complexes. For the same ligand L in $LM(CO)_5$, the trend in $\nu(CO)A_1$ is $Cr < W \leqslant Mo$. The carbonyl bands are, however, little affected by variation in L or M and do not provide a sensitive probe of the electronic effects accompanying such changes. The molecular dipole moments decrease in the order pyridine-$M(CO)_5$ > quinuclidine-$M(CO)_5$ > trimethylamine-$M(CO)_5$ for similar M; this trend parallels that of the free amine ligands. Only small increases are found in the $LM(CO)_5$ moments with change of M from Cr to W. The data are interpreted to suggest a degree of π-back bonding in the pyridine complexes but the results are by no means conclusive. Molecular polarisability anisotropies from experiment for the pyridine and *p*-substituted pyridine-$M(CO)_5$ complexes were compared with anisotropies calculated for a model in which the pyridine is σ-bonded to the metal M. In all cases a strong enhancement of polarisability was found specifically in the direction of the pyridine-M-*trans*(CO) axis. This is regarded as direct evidence for conjugative interaction between the pyridine and $M(CO)_5$ moieties and for a significant π-bond component in the connecting N–M bond. This conclusion is further illustrated and strengthened by comparing the directional polarisabilities from experiment with those predicted for the σ-bonded system. Additional though qualified support comes from comparison of bond dimensions from the X-ray crystal structure of pyridine-$Cr(CO)_5$ and that now reported for quinuclidine-$Cr(CO)_5$.

Acknowledgements

The authors acknowledge with gratitude the assistance of Dr. G. Allen and Mr. M.S. Davies with refractivity measurements.

References

1 J.E. Huheey, Inorganic Chemistry, 3rd ed., Harper and Row, Cambridge, 1983, p. 435.

2 C.S. Kraihanzel and F.A. Cotton, Inorg. Chem., 2 (1963) 533.

3 W.A.G. Graham, Inorg. Chem., 7 (1968) 315.
4 R.C. Elder, Inorg. Chem., 7 (1968) 1117.
5 R.C. Elder, Inorg. Chem., 7 (1968) 2316.
6 R.A. Brown and G.R. Dobson, Inorg. Chim. Acta, 6 (1972) 65.
7 R.J. Dennenberg and D.J. Darensbourg, Inorg. Chem., 11 (1972) 72.
8 M.A.M. Meester, R.C.J. Vriends, D.J. Stufkens and K. Vrieze, Inorg. Chim. Acta, 19 (1976) 95.
9 M.A. Weiner, A. Gin and M. Lattmań, Inorg. Chim. Acta, 24 (1977) 235.
10 D.K. Lavallee, M.D. Baughman and M.P. Phillips, J. Am. Chem. Soc., 99 (1977) 718.
11 H. Daamen and A. Oskam, Inorg. Chim. Acta, 26 (1978) 81.
12 H. Daamen, H. van der Poel, D.J. Stufkens and A. Oskam, Thermochim. Acta, 34 (1979) 69.
13 H. Van Dam, G. Boxhoorn, D.J. Stufkens and A. Oskam, Inorg. Chim. Acta, 53 (1981) L235.
14 F.A. Cotton, D.J. Darensbourg, A. Fang, B.W.S. Kolthammer, D. Reed and J.L. Thompson, Inorg. Chem., 20 (1981) 4090.
15 W. Ries, I. Bernal, M. Quast and T.A. Albright, Inorg. Chim. Acta, 83 (1984) 5.
16 B.V. Johnson, A.L. Steinmetz and P.J. Ouseph, J. Coord. Chem., 14 (1985) 103.
17 W. Strohmeier and F. Müller, Chem. Ber., 100 (1967) 2812; 102 (1969) 3608.
18 W. Strohmeier and K. Gerlach, Z. Naturforsch. B, 15 (1960) 413.
19 U. Koelle, J. Organomet. Chem., 133 (1977) 53.
20 C.G. Le Fèvre and R.J.W. Le Fèvre, in A. Weissberger (Ed.), Techniques of Chemistry, Wiley-Interscience, New York, Vol. 1, Part IIIC, 1972.
21 C.G. Le Fèvre and R.J.W. Le Fèvre, Rev. Pure Appl. Chem. (Aust.), 5 (1955) 261.
22 R.J.W. Le Fèvre, Dipole Moments, Methuen, London, 1953.
23 Enraf Nonius Structure Determination Package (SDP), Enraf Nonius, Delft, Holland, 1985.
24 G.M. Sheldrick, SHELX-76, A Program for X-ray Crystal Structure Determination, University of Cambridge, 1976.
25 International Tables for X-ray Crystallography, Kynoch Press, Birmingham, Vol. 4.
26 C.K. Johnson, ORTEP, A Thermal Ellipsoid Plotting Program, Oak Ridge National Laboratories, Oak Ridge, 1965.
27 R.E. Dessy and L. Wieczorek, J. Am. Chem. Soc., 91 (1969) 4963.
28 G. Keeling, S.F.A. Kettle and I. Paul, J. Chem. Soc. A., (1971) 3143.
29 F.T. Delbeke and G.P. van der Kelen, J. Organomet. Chem., 64 (1974) 239.
30 M.J. Aroney, R.M. Clarkson, R.J. Klepetko, A.F. Masters and R.K. Pierens, J. Organomet. Chem., 393 (1990) 371.
31 T.W. Hambley and P.A. Lay, Inorg. Chem., 25 (1986) 4553.
32 P.A. Lay, Inorg. Chem., 23 (1984) 4775.
33 R.S. Armstrong, M.J. Aroney, K.E. Calderbank and R.K. Pierens, Aust. J. Chem., 30 (1977) 1411.
34 M.J. Aroney, M.K. Cooper, R.K. Pierens and S.J. Pratten, J. Organomet. Chem., 309 (1986) 293.
35 R.J.W. Le Fèvre, Adv. Phys. Org. Chem., 3 (1965) 1.
36 C.G. Le Fèvre and R.J.W. Le Fèvre, J. Chem. Soc., (1955) 2750.
37 M.J. Aroney, M.K. Cooper, R.K. Pierens, S.J. Pratten and S.W. Filipczuk, J. Organomet. Chem., 295 (1985) 333.
38 M.J. Aroney and S.J. Pratten, J. Chem. Soc., Faraday Trans. 1, 80 (1984) 1201.
39 R.M. Finlayson, Honours B.Sc. Thesis, University of Sydney, 1986; M.Sc. Thesis, University of Sydney, 1989.
40 G.W. Allen, private communication.